



Eco-friendly dyeing and finishing of organic cotton fabric using natural dye (gardenia yellow) reduced-stabilized nanosilver: full factorial design

Huiyu Jiang · Rui Guo · Rony Mia · Heng Zhang · Shaofang Lü · Feng Yang · Sakil Mahmud · Huihong Liu

Received: 30 June 2021 / Accepted: 23 December 2021 / Published online: 24 January 2022
© The Author(s), under exclusive licence to Springer Nature B.V. 2022

Abstract Traditional coloration and functionalization of textiles are highly energy-consuming, time ineffective, and require many chemicals. To overcome the drawbacks, cost-effective and eco-friendly natural dyeing and finishing have become an urgent demand. Herein, gardenia yellow, a natural dye, is extracted from *Gardeniae fructus* seeds and used for the coloration of organic cotton fabrics (OCFs). In addition, silver nanoparticles (AgNPs) were synthesized

in-situ on the surface of the OCFs, where gardenia yellow serves as a reducing and stabilizing agent. Optimization of the process parameters (AgNO₃ conc., gardenia yellow conc., solution pH, and reaction time) for the yield of AgNPs and subsequent fixation of nanoparticles on the OCFs surface were controlled by Taguchi design of experiments. All parameters were tested in a specified range at four levels on the color strength (K/S) and color difference (ΔE) value. Structural characterization of optimized samples revealed that the AgNPs are nanometer size, spherical shapes, evenly dispersed, and firmly attached to the fiber surfaces by molecular force or double networking capabilities of plant phytochemicals. Color properties demonstrate an even shade due to the surface plasmon resonance (SPR) of AgNPs with brilliant color strength. Functional properties exposed that the *in-situ* synthesis of AgNPs significantly enhanced the UV resistance and antibacterial activity (against *Staphylococcus aureus* and *Escherichia coli*) of the OCFs. Overall, this technique of OCF coloration and functionalization by avoiding traditional chemicals including mordants, binders, crosslinkers, finishing, or coating agents offers the desired efficiency and safe product for practical application.

Supplementary Information The online version contains supplementary material available at <https://doi.org/10.1007/s10570-021-04401-9>.

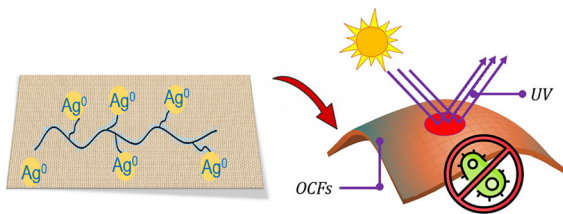
H. Jiang · R. Guo · R. Mia · S. Lü · F. Yang · S. Mahmud (✉) · H. Liu (✉)
Hubei Key Laboratory of Biomass Fibers and Eco-Dyeing & Finishing, School of Chemistry and Chemical Engineering, Wuhan Textile University, No.1 Sunshine Avenue, Jiang Xia District, Wuhan 430200, People's Republic of China
e-mail: sakilmahmud@nimte.ac.cn

H. Liu
e-mail: huihongliu@wtu.edu.cn

R. Mia · S. Mahmud
Center for Research and Industrial Relation, Department of Textile Engineering, National Institute of Textile Engineering and Research, University of Dhaka, Dhaka 1000, People's Republic of Bangladesh

H. Zhang
Inner Mongolia Erdos Resources Co., Ltd., Inner Mongolia Autonomous Region, Ordos 017000, People's Republic of China

Graphical abstract



Keywords Natural dyes · Gardenia yellow · Silver nanoparticles · Textiles · Taguchi design of experiment

Introduction

Textile and apparel industries contribute to satisfying the growing need for clothing, which is the second basic need for humans after food. One of the consumers' primary demands is colored textiles. However, a colorful appearance is typically achieved by multiple consecutive steps of wet processing. Commonly, dyes/pigments are routinely fixed by thermal/mechanical retention, physical adsorption, covalent bonds, or complexation with metals between fiber and dye molecules in the conventional wet processing method (Perkins 1996). Toxic functional groups such as methine, azo, nitro, anthraquinone, aril methane or carbonyl, etc., (commonly known as chromophore and auxochrome) present in the dye molecules are mainly responsible for imparting color (Gürses et al. 2016). Statistics show that more than 10,000 variants of dyes and pigments are used in the different manufacturing sectors, where these sectors demand over 700,000 tons/year of synthetic dyes globally (Wan et al. 2021b). Among them, about 200,000 tons/year of these dyes are discharged as effluents due to the inefficient and lengthy dyeing and finishing process in the traditional textile industry (Wan et al. 2021a). In addition, a large volume of water is required throughout the operation. An available knit-dyeing factory needs an average of 10 gallons of water for a single pound of cotton dyeing (Shaikh 2009). Besides, 1 kg of cotton dyeing requires approximately 10 g of reactive dyes, 76 g of alkali,

1.2 kg of salt, and many auxiliaries, such as leveling agent, wetting agent, sequestering agent, soda and anti-creasing agent, peroxide, etc. (Kim et al. 2017). Unfortunately, these dyes and auxiliaries are poisonous to human and other living things and pollute water sources severely, putting the aquatic ecosystem at risk in various ways. Owing to the high structural stability of dyes/pigments to sunlight, temperature, water, or other factors, they remain stable in the atmosphere year after year (Chen et al. 2020b). Again, textile materials require additional functional finishing such as antibacterial, fire resistance, UV repellency, waterproofing, or self-cleaning (Le Marechal et al. 2012; Sultana et al. 2019). These functional finishing agents are more environmentally defiant due to their complex aromatic composition and synthetic origin. As a result, minimizing water pollution and chemical use in textile dyeing and finishing has become an immediate need for a safe and sustainable world.

Usually, the extracts of various branches of plants come in the front line as natural dyes to resolve the aforementioned problems. The presence of flavonoids and natural pigments in the plant branches can express a broad spectrum of colors (Vankar 2000). Therefore, many pieces of research have been carried out in recent decades on synthesizing plant-derived natural dyes and their application for textile coloration (Samanta 2020). Likewise, we have also attempted to extract natural dye from *Macadamia integrifolia* for cotton dyeing as a potential substitute for reactive dyes (Habib et al. 2017). However, we observed both in our study (Habib et al. 2017) and other research (Samanta 2020), besides numerous advantages, natural dyes pose many limitations. For example, colors obtained from plant components are non-reproducible, highly expensive, less color yieldable, and offer poor fastness properties. Also, the necessity of excessive auxiliaries or mordants and the unavailability of technical information make them more challenging for commercial application. Hence, the organized application of greenly synthesized metal nanomaterial is a much better option for coloration and multi-functionalization of textile materials, simultaneously (Hasan et al. 2020b, c). These nanomaterials demonstrate a wide range of colors, depending on the particle size, shape, and synthesis protocol, due to their localized surface plasmon resonance (LSPR) properties (Chen et al. 2021a; Guo et al. 2021). In addition, metal ions and metal-based compounds such as silver are inherently

used to reduce at least twelve species of bacteria and highly toxic microorganisms due to the biocidal action of silver leaching (Mahmud et al. 2018; Ru et al. 2018). With the utilization of these features of nanomaterials, a simple one-step treatment can enhance both functional properties and the colorful appearance of textiles (Hasan et al. 2019, 2020a). Therefore, the nanomaterials have been applied to the fabric substrates using sol–gel, *in-situ* deposition, dipping-coating, and padding methods for textile treatment (Rehan et al. 2019; Yu et al. 2019). Besides the applications in textiles coloration and antibacterial finishing, nanomaterials are widely used in optical sensors, biomedical fields, chemical industries, drug-gene delivery, transistors, photo-electrochemical, catalysis, light emissions, cosmetics, and other important areas (Marin et al. 2015; Natsuki et al. 2015). Unfortunately, these broader applications are hindered by the aggregation and agglomeration tendency of nanoparticles (Rao et al. 2020; Shahid ul et al. 2020). The chemical reduction method, in this regard, requires toxic chemicals and cannot serve alone as a simultaneous reducing and stabilizing agent to stop agglomeration completely (Chen et al. 2021a; Iravani et al. 2014; Wang et al. 2022). To prevent particles agglomeration in a green synthesis protocol, naturally derived reducing and stabilizing agents are essentially required (Chen et al. 2021b; Xiong et al. 2020, 2021). Plant phytochemicals, polysaccharides, and other carbohydrates sources are decent choices in this respect and can serve as a supplementary template for the colloidal synthesis of metal nanoparticles (Huang et al. 2019; Thangaraj et al. 2017; Wang et al. 2021). Gardenia (*Gardenia jasminoides*) is a plant widely used in medicine, food colorant, and various health supplements. The water-soluble carotenoid fraction in gardenia, which principally contains crocin and crocetin, is mainly referred to as gardenia yellow (Xu et al. 2016). Although gardenia yellow dyes were previously extracted, their application in reducing and stabilizing silver nanoparticles (AgNPs) via *in-situ* synthesis on the organic cotton fabrics (OCFs) for coloration and simultaneous functionalization was not explored.

It is worth pointing out that organic cotton is the primary raw material for enhancing textile sustainability. It gets its name from the fact that it is grown naturally without industrial agrochemicals such as fertilizers, pesticides, or transgenic techniques

(Guerena and Sullivan 2003). Traditional chemicals including, herbicides, growth regulators, insecticides, and defoliants, are prohibited from being used for at least three years before organic cotton filed. It stimulates biodiversity, supports ecological processes, and protects human health and the environment (Rieple and Singh 2010). In contrast, cotton grown conventionally uses far too many pesticides and crop protecting chemicals, causing several environmental problems. Furthermore, since the danger of cancer has grown, customers are becoming more concerned about the raw materials used in end-products that do not include any chemical residues. Aside from the tremendous benefits, there are certain difficulties to overcome, such as the mechanical properties of organic cotton is inferior to standard cotton (Mahmud et al. 2020). For example, Sanches et al. (2014) reported knitted fabrics prepared from different natural/blend fibers, including organic cotton. They evaluated the pilling properties, elasticity, rupture pressure, moisture absorption, elongation, and dimensional stability. Results emphasized that the fabrics manufactured other than organic cotton displayed better performance. Chae et al. (2011) investigated the mechanical properties of organic cotton in terms of tactile sensory perceptions and compared it with other fibers. The report revealed that different fibers had substantial variations in surface, shear, compression characteristics, and weight. Thus, we are reporting here modifying organic cotton to impart natural color, increase bacterial resistance, and induce UV protection to create genuinely sustainable materials.

Like other traditional wet processing, nanomaterial assisted dyeing/finishing of textile is significantly influenced by several factors that require optimization, including the concentration of metal precursor, the concentration of reducing/stabilizing agent, the pH of the reaction bath, and the incubation time. One-factor-at-a-time is studied in the traditional optimization process while keeping all other conditions constant (Mahmud et al. 2017b, 2019). Consequently, this process does not evaluate cross-effects among the factors and leads to an insignificant optimization. While a process contains multiple factors, it is logical to adopt statistical-based optimization methods to achieve the aforementioned objects. A statistical-based experimental design is a modern technique; where all the variables or parameters were simultaneously studied in a specified range using a few

experiments to acquire systematic outputs or signals for further analysis (Shafiq et al. 2018). The Taguchi design of experiment (DoE) is such a technique that can be used in process optimization and simultaneously in performance improvement (Morshed et al. 2020). Even the DoE can also rank the factors according to their contribution to process/product and development (Cai et al. 2020). To the best of our knowledge, no study has reported the statistical modeling and optimization of the dyeing and finishing process of organic cotton using natural dye mediated nanoparticles through a full factorial design.

Therefore, this study used an L^{16} orthogonal array of four parameters and four levels full factorial experimental design to optimize the dyeing and finishing process. Individual and interaction effects of incubation time, solution pH, and silver nitrated/gardenia yellow concentration were studied in statistical modeling. The responses (outputs) considered were the color strength (K/S value) and color differences (ΔE value) as an indication of successful coloration and functionalization of OCFs. In this Taguchi technique, a signal-to-noise ratio (S/N) was calculated to obtain optimal parameters from the response table for significance screening of the specific factor. Lately, a confirmation test has been deployed to validate the DoE concerning practical viability. The samples prepared based on the optimized conditions from the statistical results were structurally characterized to observe the morphological change caused by the deposition of AgNPs. Other important properties of synthesized AgNPs, such as crystal structure, particle size, homogeneity of distribution, and surface charge, were also studied. A mechanism of the ternary interaction among organic cotton, nanosilver, and plant phytochemicals was explored. Samples' functionality in terms of UV protection and bacterial resistivity was evaluated using a recognized standard method.

Experimental

Materials

Certified bleached organic cotton fabrics (OCFs, 1/1 plain weave construction, weight density = 128 g/m², and yarn density = 120 ends/inch and 70 picks/inch) were supplied by Henan Pingmian Textile Group Co.,

Ltd. (Pingdingshan, China). Silver nitrate (AgNO₃) and sodium hydroxide (NaOH) in the analytical grade were purchased from Sinopharm Chemical Reagent Co., Ltd. (Shanghai, China) and used as received. The *Gardenia fructus* seeds were purchased from Huacaoyun Biotechnology Co., Ltd., Bozhou, Aihui, China.

Preparation of natural dyes (gardenia yellow)

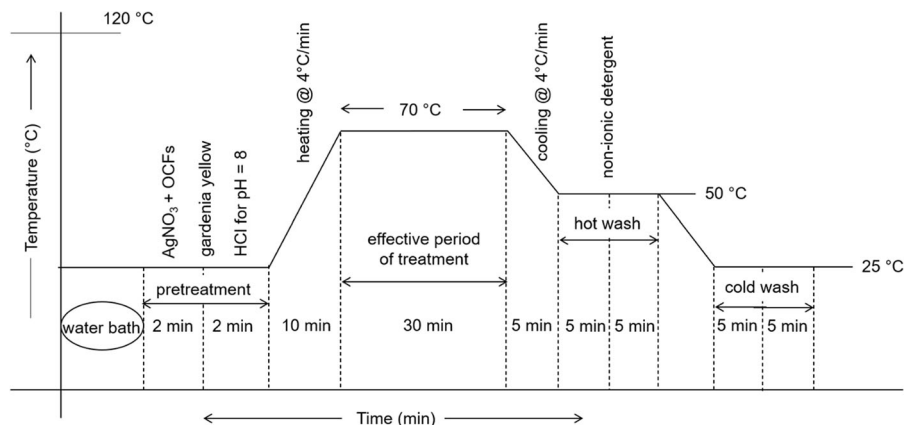
According to the available method with minor modifications, the gardenia yellow was extracted from *Gardenia fructus* seeds (Saravanakumar et al. 2018). In brief, the seeds were crushed at a rotation speed of approximately 10,000 rpm using a conventional pulverizer (IFM-800DG, Iwatani Corp., Japan) to prepare fine powder. About 10 g of as-prepared powder was dissolved in 250 mL of deionized water maintaining solution pH = 12 and boiled in an oscillator with water bath in constant temperature at 80 °C for 2 h to get a crude extract of gardenia yellow. Finally, the extract was filtered through Whatman No.1 filter paper, and then the filtrate was collected in a 250 mL Erlenmeyer flask and stored at room temperature for subsequent use.

AgNPs assisted dyeing/finishing of OCFs

Bleached OCFs (2.0 g) were immersed into a 250 mL Erlenmeyer flask containing a solution of 10 mM AgNO₃ (10 mL) and deionized water (70 mL) for the adsorption and dispersion of Ag⁺. Natural dyes of 20 mL were induced to the flask with maintaining the pH = 8 (using hydrochloric acid) and heated the flax at 70 °C for 30 min. The OCF samples were washed with and without a non-ionic detergent (1 g/L) to remove the unfixed nano-ingredients with a materials-to-liquor ratio of 1:60 (w/v) at 50 °C for 10 min and then dried sufficiently at 60 °C in a thermostatic vacuum drier. The step-by-step functionalization via exhaust method is presented in the process curve (Scheme 1). Here, the resulting OCFs have been designated as 'AgNP dyed OCFs'.

Design of experiment (DoE)

The Taguchi design of experiments is an experimental setting used to analyze the impact of multiple factors of multiple levels to achieve an optimum output by



Scheme 1 The process curve of step-by-step OCF functionalization using nanosilver

employing a minimum number of trials (Pervez et al. 2018). Since we have used four levels of four control parameters (AgNO_3 conc., solution pH, plant extract conc., and reaction time) (Table 1), an L^{16} orthogonal array of factors was chosen to obtain the maximum number of trials (Table 2). Finally, each trial's outputs (ΔE and K/S) were systematically analyzed using the signal-to-noise (S/N) ratio (Text S1: Supplementary Information), interaction plots, residual plots, confirmatory/validation test, and a response table. A Minitab 19 software was used to analyze and plot the data, according to Pervez et al. (2018).

Characterization and measurement

The surface morphology of control and AgNP dyed OCFs were observed by scanning electron microscopy (SEM, JEOL 7800F, Tokyo, Japan). The elemental composition of AgNPs deposited on the OCFs surface was analyzed using energy-dispersive X-ray (EDX) equipped with SEM instruments. The InCA automated and mapping software was used for the initial data collection and image processing. The particle shape

and size distribution of the AgNP dyed OCFs was observed by a transmission electron microscope (TEM, JEOL-JEM-2100F, Tokyo, Japan) at an accelerating voltage of 20 kV. The crystallinity phase of AgNP dyed OCFs was characterized by X-ray diffraction (XRD, Bruker D8 Advance Diffractometer, Bruker AXS, Germany) with $\text{Cu K}\alpha$ radiation ($k = 0.154 \text{ nm}$) in the range of $5^\circ\text{--}80^\circ$ (2θ) at 40 keV. Herein, AgNP dyed OCFs were put in a 50 ml glass bottle with 50 ml of water. The bottle was centrifuged at 6000 rpm for 30 min to enable enough time for the OCFs to leach AgNPs. The OCFs were then removed, and the residual water was squeezed out into a glass container. The AgNP-containing centrifuged water was used for the TEM and XRD analysis. The surface zeta potential and average size distribution of the particle (after extraction from AgNP dyed OCFs followed by solution extraction using centrifuge) were determined using Zetasizer (Nano-ZS90, Malvern Instruments, UK).

The color yield of the AgNP dyed OCFs in terms of CIE $L^*a^*b^*$ values and color strength (K/S) based on the Kubelka–Munk equation were evaluated by the

Table 1 Parameters and their levels

Symbol	Process Parameters	Level 1	Level 2	Level 3	Level 4
A	AgNO_3 conc. (mM)	1*	2*	3*	4*
B	Solution pH	04	06	08	10
C	Extract conc. (mL)	06	12	18	24
D	Reaction time (min)	40	50	60	70

*1, 2, 3, and 4 are denoted as 0.25, 0.50, 1.0, and 2.0 mM AgNO_3 , respectively

Table 2 Experimental layout using L¹⁶ orthogonal array of factors, experimental data, and their S/N ratios

Trail no.	A	B	C	D	L	A	B	ΔE	S/N Ratio (dB)	K/S	S/N Ratio (dB)
1	1	1	1	1	90.89	−0.65	16.49	12.90	22.212	0.1643	−15.687
2	1	2	2	2	88.34	−0.11	32.43	29.00	29.248	0.5508	−5.180
3	1	3	3	3	89.94	−1.24	35.25	31.50	29.966	0.5368	−5.404
4	1	4	4	4	88.04	1.91	31.62	28.40	29.066	0.4486	−6.963
5	2	1	2	3	90.77	−0.82	24.31	20.60	26.277	0.2754	−11.201
6	2	2	1	4	86.64	2.82	33.24	30.40	29.658	0.6327	−3.976
7	2	3	4	1	90.19	−1.81	34.63	30.90	29.799	0.5188	−5.700
8	2	4	3	2	90.13	−1.48	34.93	31.20	29.883	0.526	−5.580
9	3	1	3	4	81.91	2.82	31.25	30.10	29.571	0.829	−1.629
10	3	2	4	3	89.44	−0.28	32.67	29.10	29.278	0.4863	−6.262
11	3	3	1	2	88.58	−1.50	33.23	29.80	29.484	0.5525	−5.153
12	3	4	2	1	88.82	0.34	32.96	29.50	29.396	0.5261	−5.579
13	4	1	4	2	88.96	0.53	29.44	26.00	28.300	0.4313	−7.304
14	4	2	3	1	89.65	0.52	28.72	25.20	28.028	0.3889	−8.203
15	4	3	2	4	90.54	−2.23	33.44	29.70	29.455	0.4787	−6.399
16	4	4	1	3	88.43	−0.24	29.81	26.50	28.465	0.4798	−6.379

light reflectance technique (Text S2: Supplementary Information). Colorfastness washing, light, and rubbing was determined according to the standard of ISO 105-C02 (1989), ISO 105-X12 (1987), and ISO 105-B02 (1988), respectively (Text S3: Supplementary Information). Antibacterial were performed using agar disk diffusion as described in Text S4: Supplementary Information. The UV transmission spectra of AgNP dyed OCFs were measured using a UV/Vis spectrophotometer (Analytikjena, Germany). The ultraviolet protection factor (UPF) values were automatically calculated using a Startek UV fabric protection application software (Startek Technology, version 3.0).

Result and discussion

Statistical modeling and optimization

AgNPs enhance the intensity and brilliance of colors on the substance without traditional dyes due to their localized surface plasmon resonance (LSPR) properties (Mahmud et al. 2017a). The photograph of the OCF samples before and after *in-situ* synthesis of AgNPs are showed in Fig. 1. It can be observed that the OCF sample color changed from off-white/grey to

yellow due to the incorporation of AgNPs. The color strength (K/S) value is typically measured to understand the color content of the dyed materials (Pervez et al. 2017). Therefore, optimizing the K/S value of the AgNP dyed OCFs by adjusting the variable process parameters is ultimately the optimization of AgNP incorporation. Regarding the appearance of yellow shade, the K/S values were recorded at 425 nm wavelength. Similarly, the color difference (ΔE) for AgNP dyed OCFs is an effect of AgNPs on the color of OCFs samples. The ΔE values were measured according to the CIE Lab coordination system using a standard equation (Text S2: Supplementary Information). Increasing the ΔE values laterally increasing the AgNP deposition on the OCFs surface. Therefore, the optimization of ΔE values by studying variable process parameters was achieved as an indication of optimum AgNP incorporation on the OCFs surfaces.

An L¹⁶ orthogonal Taguchi design of experiment was used to achieve the optimum parameters for the highest outputs for ΔE and K/S values (Table 2). In this DoE, the S/N ratio was considered to measure desirable/non-desirable levels of the experiment. Since the outputs have a proportional correlation in terms of AgNPs on the OCFs, the ‘larger-the-better’ function (higher the response value, the better the outputs) was selected to estimate the optimum level.

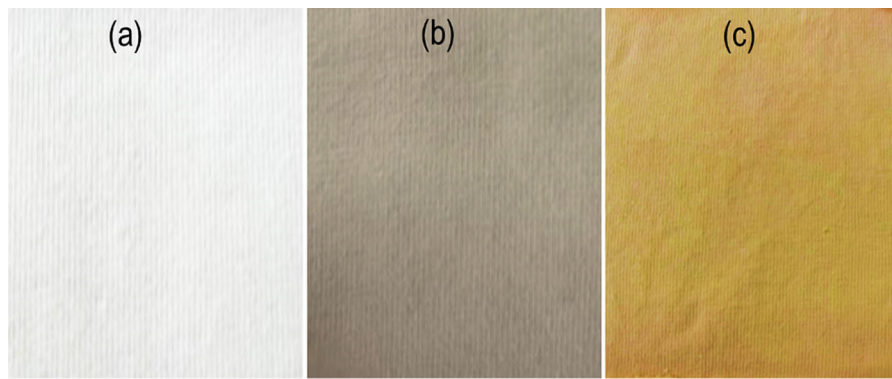


Fig. 1 Photographs of (a) control OCFs, (b) gardenia yellow treated OCFs and (c) gardenia yellow mediated AgNP dyed OCFs

The optimal AgNP fixation with regard to the output was determined by the obtained results and subsequently used for delta statistic value (the difference between the highest mean value and the lowest mean value of a particular parameter) (Table 3). The calculated delta values are arranged in an arithmetic series beginning from rank 1 to rank N. The highest value indicates rank 1, and the lowest value indicates rank N in ascending order. Concerning the ΔE values (Table 3: a), the pH substantially influences the AgNP fixation; hence, it was denoted as rank 1. This was followed by reaction time, extract conc., and AgNO₃ conc., contributed as rank 2, rank 3, and rank 4, respectively. Similarly, the delta statistical analysis regarding the K/S (Table 3: b) indicates that the reaction time has the highest influences (rank 1) on the AgNP fixation followed by the AgNO₃ conc., the solution pH, and the extract conc.

The main effect plot produced by the S/N ratio defines the influence of the individual independent parameters on the dependent parameters across all levels (Fig. 2). The overall scenario of the factor's

impact on the process can be perceived by evaluating the main effects of the parameters (Shafiq et al. 2018). In Fig. 2a, the main effect plots for the S/N ratio (ΔE) show that the third level of AgNO₃ conc. (A₃), solution pH (B₃), and extract conc. (C₃), as well as the second level of reaction time (D₂) revealed the optimum values of ΔE . Similarly, another main effect plot was produced for K/S values originated S/N ratios (Fig. 2b). It can be again observed that the third level of AgNO₃ conc. (A₃), solution pH (B₃), and extract conc. (C₃), and the second level of reaction time (D₂) were revealed as optimum results of the K/S. Both plots are consistent with the S/N ratio analysis (Table 3), indicating that the same levels of the parameters (A₃, B₃, C₃, and D₂) are nominated for the highest AgNP fixation employing maximum ΔE and K/S values and referred to as optimized condition.

The interaction plots are mainly produced to recognize the occurrence of interactions among variable process parameters (Cai et al. 2020). In such plots, the interactions are generally found by a set of parallel lines (weak/absence of relationships) or a set

Table 3 Response table for signal to noise (S/N) ratios: (a) ΔE and (b) K/S (larger is better)

Level	(a) S/N ratios for the response of ΔE				(b) S/N ratios for the response of K/S			
	A: AgNO ₃ conc	B: pH	C: Extract conc	D: Time	A: AgNO ₃ conc	B: pH	C: Extract conc	D: Time
1	27.62	26.59	27.45	27.36	−8.308	−8.955	−7.799	−8.792
2	28.90	29.05	28.59	29.23	−6.614	−5.905	−7.090	−5.805
3	29.43	29.68	29.36	28.50	−4.656	−5.664	−5.204	−7.311
4	28.56	29.20	29.11	29.44	−7.071	−6.125	−6.557	−4.742
Delta	1.81	3.09	1.91	2.08	3.653	3.291	2.595	4.051
Rank	4	1	3	2	2	3	4	1

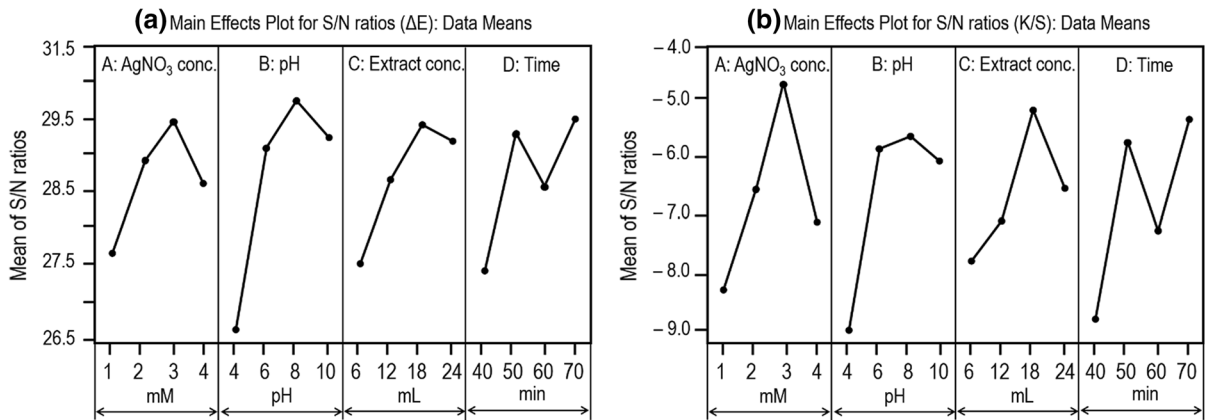


Fig. 2 Main effect plots for S/N ratios, response: (a) ΔE and (b) K/S value (herein, signal-to-noise: larger is better)

of non-parallel lines (presence of relationships) among process parameters for a given set of experimental arrays. The interaction plots for ΔE based S/N ratios demonstrate that all four factors (A, B, C, and D) strongly intersect, i.e., a non-parallel nature of lines indicating the occurrence of a complex cross interaction among these four factors (Fig. 3a). Similar phenomena are also observed in the interaction plots for K/S value originated S/N ratios (Fig. 3b). Cai et al. (2020) also observed identical characteristics in the interaction plots during the reactive dye fixation on ramie fiber in liquid ammonia. Collectively, it could be concluded that the designated factors had a significant impact on the AgNP fixation.

The residual plots are produced in the responses of ΔE and K/S values using their corresponding S/N ratios (Figure S1: Supplementary Information). Each plot is typically consisting of four components, including (i) normal probability plot, (ii) histogram, (iii) residuals vs. fitted values plot, and (iv) residuals vs. observation order. It is evident that the plots of normal probability are mostly linear for both responses, where almost all points are pointed on the line or around the line. Hence, it is inevitable that the errors are typically distributed during the fixation of AgNPs. The histogram bar chart further ensures this normal distribution. However, the residuals vs. fitted values plot demonstrates that the error points are almost equally dispersed in both the upper and lower

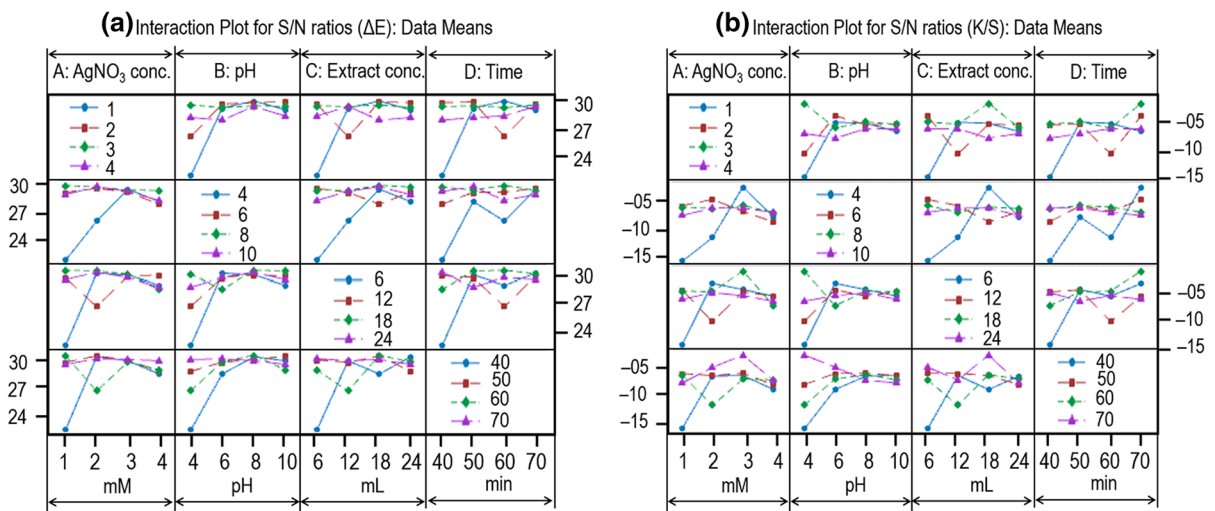


Fig. 3 Interaction plots for S/N ratios: (a) ΔE and (b) K/S value

portion of the zero lines, representing a constant variance significance. Likewise, the residuals vs. the observation order plot reveal that the error points are casually encountered around the zero-line. It indicates that the residuals depend on the AgNP fixation to analyze the pattern that influence the responses (ΔE and K/S). In summary, the responses expose that the residuals are in uniform distribution on both sides of the zero line, which implies that the results are mutually agreeable and do not require any additional investigation of the errors analysis (Hossain et al. 2021).

The regression equation was produced to perfectly estimate the predicted values based on the experimental design and then compared the predicted values with the observed/actual value (Morshed et al. 2020). Figure 4 displays the linear fitted plots of the predicted vs. actual value in response to ΔE and K/S. The plot indicates that the DoE was significant since the line is firmly fitted for the predicted vs. actual value in response to ΔE and K/S. In addition, the fitting rate constants (R^2) were calculated to 98.4% and 91.2% with adjusted R^2 of 98.3% and 91.7% in the response of ΔE and K/S, respectively. The values are thus in strong agreement with each other. Also, a p -value of 0.000 for both responses indicate a significant relationship between predicted and actual values.

Characterizations of AgNP treated OCFs

The reduction of silver ions and stabilization of AgNPs were achieved via the reduction and stabilization capability of plant phytochemicals. Herein, the gardenia yellow has played at least three roles: (i) gardenia phytochemicals can serve as reducing agents for the reduction of silver cation to neutral ion; (ii) after successful reduction, they keep the produced AgNPs stable by creating a thin layer of cladding over the particles; (iii) finally, the thin layer of cladding (of gardenia phytochemicals) over the particles serves as a bridging agent to bind the AgNPs on the OCFs surface. The potential mechanism of AgNP formation on OCFs is presented in Scheme 2. The concept was adapted from recently published articles regarding the *in-situ* green synthesis of AgNPs on cotton fibers using phytochemicals of other plants (Čuk et al. 2021). The heavy metal adsorption capability and physical stability are what lead to the adoption of silver cation (Ag^+) by the cellulose surface while the OCFs are immersed in AgNO_3 solution. Thereby, the Ag^+ can be bound to cellulose structure by an ion–dipole interaction. Even if the cotton fabric is left in the AgNO_3 solution for a few days, the nanoparticles will not form if the silver cation reduction process is not continued (Yazdanshenas and Shateri-Khalilabad 2012). To prove the concept, OCFs were immersed in AgNO_3 solution (without gardenia extract) for 30 min at 70 °C; and it has yielded no visible color on the OCFs surface (Fig. 1), indicating the absence of AgNP formation.

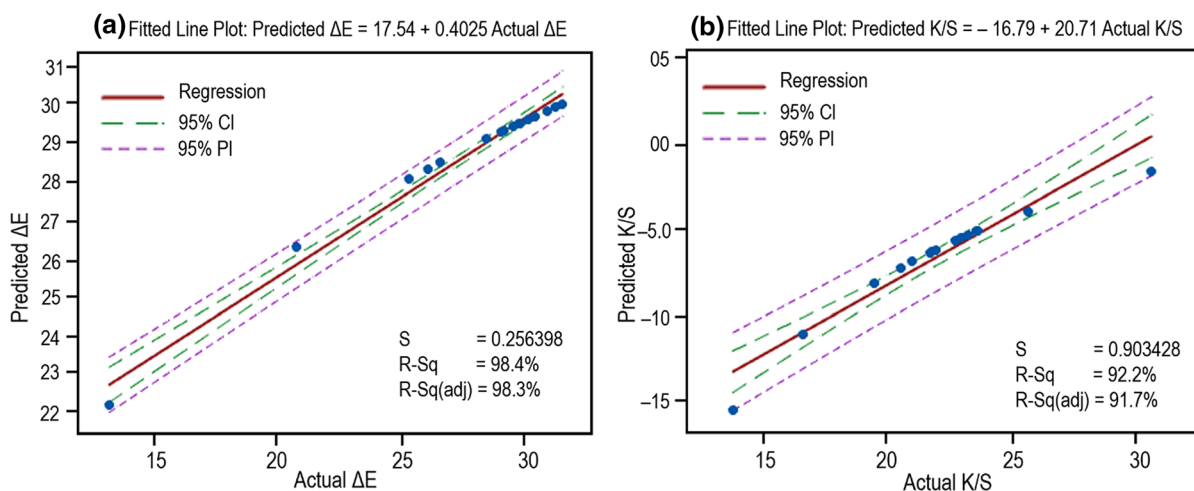
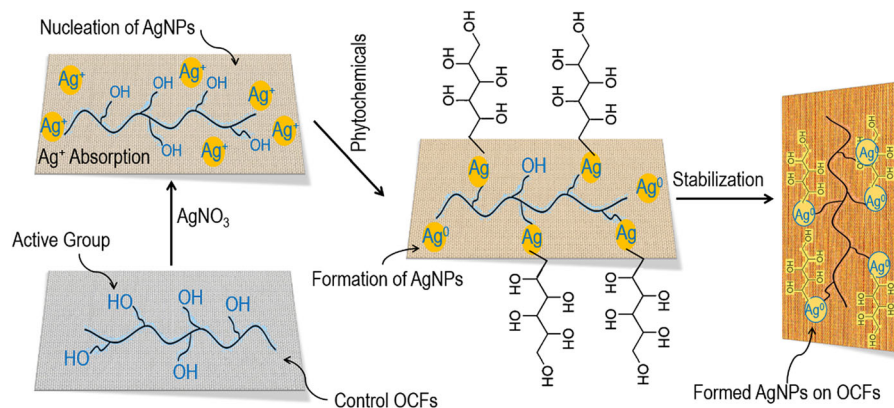


Fig. 4 Fitted lines for the actual and predicted values: (a) ΔE and (b) K/S value



Scheme 2 Possible chemical reactions during in-situ synthesis of AgNPs on OCFs

Whatever the technique employed for green synthesis, the macromolecules in the plant extract (such as polyphenols and flavonoids) are mainly responsible for controlling the generation and stabilization of AgNPs. Gardenia yellow also contains iridoids, carotenoids (crocin), monoterpenoids and their glycosides, flavonoids, organic acid esters, and sterols (Cai et al. 2015). Like other plant phytochemicals (Liu et al. 2020), these constituents are responsible for reducing Ag^+ and stabilizing AgNPs. In this technique, water-soluble parts of gardenia yellow (e.g., D-glucose) were initially dispersed over the silver absorbed OCFs to form a ternary complex $[\text{OCFs}-\text{Ag}(\text{gardenia yellow})]^+$, and then further reaction with the OH^- ions to form AgNPs by the reduction of silver cations through the oxidation to gluconic acid (Vasireddy et al. 2012). Moreover, successful fixation of AgNPs on the OCFs surface may be achieved in two ways. (1) Comparatively bigger AgNPs are entrapped inside the fibril/fiber network of the OCFs surface and then tightly attached to the fiber surface through molecular force generated by the thin layers of plant phytochemicals molecules over the particles (Hasan et al. 2020b). (2) Osmotic pressure penetrates the comparatively smaller AgNPs through the fibroporous system and becomes entangled by the double network of plant phytochemicals (Hasan et al. 2020c). In summary, the hydroxyl or carbonyl groups on the surface of OCF can act as ligands and are capable of bonding with nanosilver. Similarly, organic groups in natural dye molecules also have the ability to interact with AgNPs. The growth of nanosilver seeds and their *in-situ* deposition and fixation on the OCFs are shown in Scheme 2. Although there were multiple ingredients

of gardenia phytochemicals responsible for establishing the interaction between OCFs and AgNPs, as a most effective component (Tavaf et al. 2015), D-glucose has been shown to represent other components.

The surface morphology of control OCFs and AgNP dyed OCFs samples were captured by a typical SEM instrument (Fig. 5b₁–b₂). It was observed that the surface of the control OCFs was very smooth when touched. However, the changes in the OCFs microscopic surface caused by the generation and immobilization of AgNPs were significant. The AgNP dyed OCFs demonstrate a somewhat rough and uneven surface due to the successful immobilization of AgNPs on the fiber surface. The surface also exhibits a compact coating with AgNPs clusters, proving that the AgNPs were loaded on the OCFs fiber. However, the process neither damages the structure of particles nor the fiber structure. The SEM-assisted EDX was used to investigate the fundamental information regarding the chemical composition of the AgNP deposited on the OCFs surface (Fig. 5a). The linear scanning revealed a clear presence of the Ag peak at 2.96 keV, representing that the Ag has been correctly recognized and exists in the OCFs surface. In addition, the visible color variance in the elemental mapping images further approves the presence of AgNPs with uniform distribution (Fig. 5c₁–c₆). Other band signals due to carbon, oxygen, nitrogen atoms, etc., are also found both in the mapping images and elemental line scan. They are revealed from the plant phytochemicals coating of the AgNPs and cellulose macromolecules (Hasan et al. 2020c). The XRD pattern of AgNPs was studied in the 2θ range of 30° – 70° to evaluate the crystal structure (Fig. 6a). Successful synthesis and

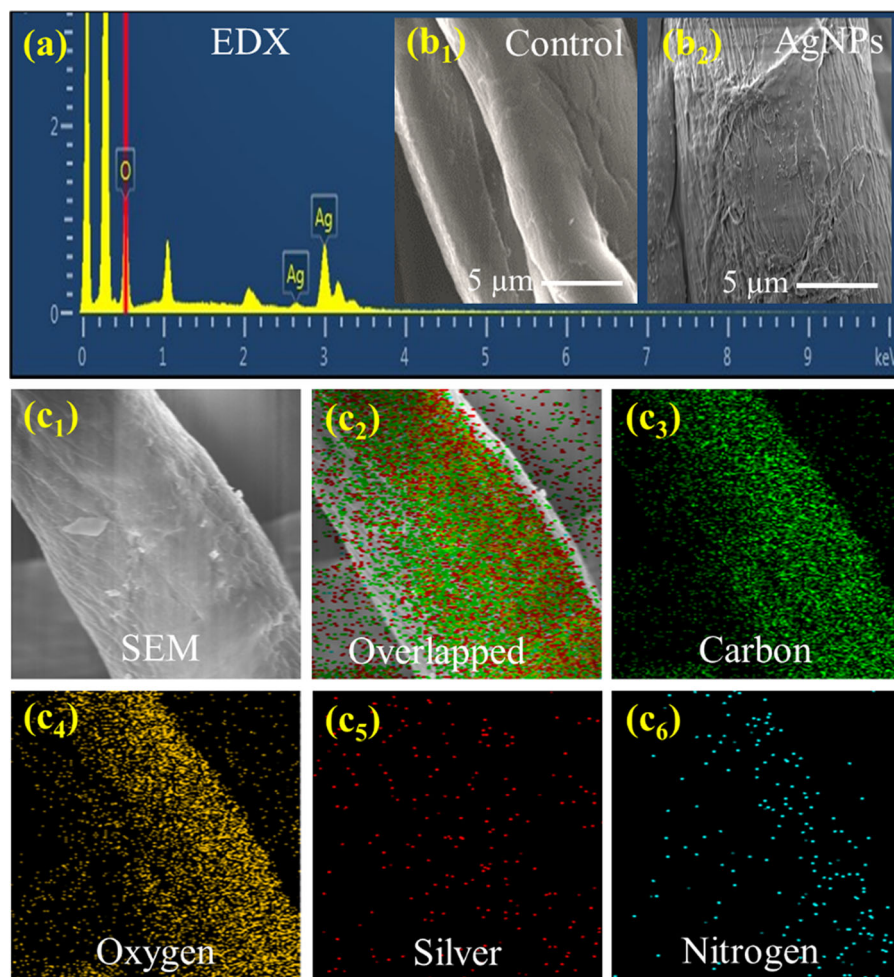


Fig. 5 (a) EDX linear scanning, (b₁–b₂) SEM images, and (c₁–c₆) SEM-derived elemental mapping images

deposition of AgNPs on the OCF surface were evidenced by the presence of the 2θ peaks at 38.1, 44.3, 64.4, and 77.5 corresponding to reflections from the (111), (200), (220), and (311) crystallographic planes of silver with face-centered cubic (FCC) structure, respectively (PDF#04-0783). The intensity of the unsplit (111) peak was noted to be dominated one, indicating that the (111) is the primary orientation of AgNPs, followed by the (200), (220), and (311) facets. The average crystal size of the AgNPs was estimated to be around 16.08 nm using the Scherrer equation (Aladpoosh et al. 2014).

The AgNP-containing centrifuged water was used for the XRD, TEM, DLS, and zeta potential analysis to understand the ultimate features of the individual nanoparticle on the OCF surface. According to the TEM observation, AgNPs were almost spherical in

shape, uniform in size, the nominal level of aggregations, and the size does not exceed 14 nm (Fig. 6d). However, the DLS measurement revealed that the particles were narrow in distribution with an average of 22.5 ± 5.2 nm. It is worth pointing that the size measured by DLS is larger than the one by TEM. This is due to the difference of measuring principles between DLS and TEM. The size measured by DLS is the size of AgNPs plus the phytochemicals bounding to the surface of AgNPs, whereas the size measured by TEM is the size of bare AgNPs. Zeta potential (ZP) of the AgNPs was estimated to be -29.0 mV, indicating the excellent stability of particles without apparent aggregation. Electronegative functional groups in gardenia yellow are responsible for the negative ZP value, suggesting that plant phytochemicals uniformly covered the nanoparticles.

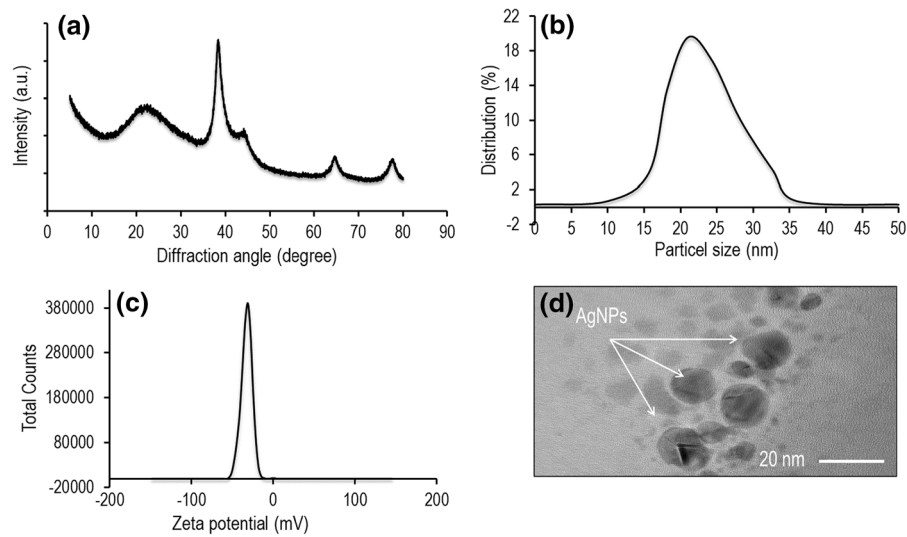


Fig. 6 (a) XRD pattern, (b) particle size distribution, (c) zeta potential, and (d) TEM micrograph of AgNPs

Another research found that a stable nano-colloidal structure can be accomplished by controlling the ZP value between -30 mV and $+30$ mV (Gengan et al. 2013). The negative charge on the nanoparticle surface in this range would produce a strong repulsive force (which prevents any van der Waals attraction) that prevents aggregation and sedimentation (Chen et al. 2020a).

Colorfastness of AgNP treated OCFs

Samples were prepared according to the as-obtained optimum condition and tested for colorfastness to explain the color properties of treated OCFs. It is worth pointing that the color of treated OCFs changes from grey/white to various degrees (shade) of yellow/brown by the optical properties of AgNPs. However, the dyeing of textile materials is not only imparting the color but also withstanding of imparted color under certain conditions. Hence, the withstanding of the imparted color on the OCF surface was evaluated by the colorfastness to washing (CFW), light (CFL), and rubbing (CFR). The results show that both CFW and CFL have a rating between 4 and 5, indicating ‘good’ color stability against wash and light, respectively. It suggests that the color of dyed OCFs is significantly withstanding the laundering and does not participate in photo-degradation while exposed to sunlight. Similarly, the CFR rating under dry and wet conditions was 3–4, indicating ‘average’ to ‘good’ color stability

against rubbing conditions. As per the Chinese National Standards for Textiles, the overall ratings are acceptable and fulfill industrial requirements (Hasan et al. 2019). The durable interactions between phytochemicals cladding (over the particles) and the functional groups of OCFs ($-\text{OH}$, $-\text{COOH}$) were principally responsible for the good fastness properties. Thus, the recommended simple coloration method allows for the dyeing of OCFs with good fastness qualities without the need of additional chemicals such as binders, crosslinkers, or coating reagents.

UV resistant of AgNP treated OCFs

The UV protection of OCFs is determined by their structure, preparation process, dyes/pigments, the presence of finishing agents, etc. UV protection is measured using the ultraviolet protection factor (UPF), which can be defined as the ability of materials to block the solar ultraviolet radiation. This value is calculated by the mean percentage of UVA (320–400 nm) and UVB (290–320 nm). The values of UPF and transmittance of light percentage for UV (UVA and UVB) of different dyed OCFs are summarized in Table 4. The higher UPF value indicates better protection against UV radiation. The results showed that the UPF value of gardenia yellow-treated OCFs was 21.15, indicating nominal protection against UV radiation. It is evident that UV was frequently passed

Table 4 UV protection properties of gardenia and gardenia-AgNP treated fabric

Samples	UPF	UVA (%)	UVB (%)
OCFs/gardenia	21.15	8.51	3.66
OCFs/gardenia-AgNPs 1 mM	42.45	2.78	2.00
OCFs/gardenia-AgNPs 2 mM	48.50	2.07	1.78

through OCFs and that their UV protection was inadequate. Indeed, the OCF dyed with gardenia-AgNP (1 mM) showed a UPF value of 42.45, indicating an excellent UV radiation blocking ability. With the increase of AgNP concentration in the OCFs, the gardenia-AgNP (2 mM) sample showed an increased UPF value, i.e., 48.50. According to the previous report, the UPF value of more than 40 and the UVA value of less than 5% is considered excellent protection against UV radiation (Shateri-Khalilabad et al. 2017). It means the result demonstrated for as-prepared samples provides outstanding UV protection. In addition, it is well known that the lower the transmittance percentage, the better the UV protection of fabrics. As shown in Table 4, the transmittance percentages of different UV regions show a reduced value due to the AgNP treatment of OCFs. It further indicates the UV blocking ability. This is possible for low transmittance of AgNP dyed OCFs due to LSPR characteristics and UV scattering for the large refractive index property of AgNPs (Gorenšek and Recelj 2007).

Antibacterial function of AgNP dyed OCFs

One of the primary objects of this study was to prepare antibacterial OCFs using *in-situ* synthesized AgNPs. Therefore, the antibacterial performances of the AgNP dyed OCFs were estimated against the gram-negative (*E. coli*) and gram-positive (*S. aureus*) bacteria. The bacterial inhibition efficiency was evaluated using zone of inhibition techniques, i.e., agar disk diffusion test. According to the test method, all samples were placed in bacteria inoculated agar plates after five washing cycles. The size for the zone of inhibition in the agar plate is shown in Fig. 7a–b. It is noticed that gardenia yellow treated OCFs show no evident inhibition zone against *E. coli* and *S. aureus* bacteria. Moreover, gardenia yellow alone cannot serve as an

antibacterial agent for OCFs. On the contrary, the AgNP dyed OCFs showed a promising antibacterial efficiency for *E. coli* and *S. aureus*, where the zones of inhibition were 7.98 ± 0.79 mm and 10.08 ± 1.18 mm, respectively. Herein, *S. aureus* showed higher sensitivity to AgNPs than *E. coli*, and it mainly depends on the bacterial structure (including anatomy and physiology), metabolism, and interaction with AgNPs charged with different reducing/stabilizing molecules (Durán et al. 2016). It is worth mentioning that the inhibition zone is bigger than the diameter of the OCFs because AgNPs and Ag^+ can migrate or diffuse through the agar hydrogel by the electrostatic attraction or the concentration gradient. From this point of view, we have tried these types of experiments to expect the anchoring of AgNPs on fiber, not only by the active groups on the surface of OCFs but also by the dye molecules. However, it was calculated (Text S2: Supplementary Information) to be more than 96% bacterial reduction for both bacterial strains, where 70% bacterial reduction is enough to meet the commercial standard of GB/T 20,944.3–2008 (Zhou et al. 2021). For further comparative analysis, *gentamicin* and *ampicillin* were used as a control for *E. coli* and *S. aureus*, respectively. As expected, *gentamicin* and *ampicillin*-treated OCFs showed a remarkable inhibition zone (i.e., 11.39 ± 0.38 mm and 13.23 ± 1.09 mm, respectively) and the results were very close to the AgNP dyed OCFs. It means the AgNP dyed OCFs have a competitive antibacterial function and meet the commercial standard requirements, which is desirable for practical applications. Several articles for AgNPs' antibacterial activities have been reported, but the exact mechanism is still unknown (Zhang et al. 2021). Based on the available literature, when the bacteria contact the AgNP dyed OCFs, the AgNPs or silver ions are released to attach to the bacterial cell membrane first and then penetrate inside the cells forming pits. Due to the superior sensitivity towards the oxygen (O_2), the neutral silver ion (Ag^0) was converted into silver cation (Ag^+) by oxidation (Tian et al. 2020). Therefore, an electrostatic attraction can be achieved between the positive charge of silver and the negative charge of the microbial cell membrane. This interaction leads to the morphological changes of membrane structure. Then membrane depolarization occurred which causes disruptions of membrane permeability and respiratory functions. As a result,

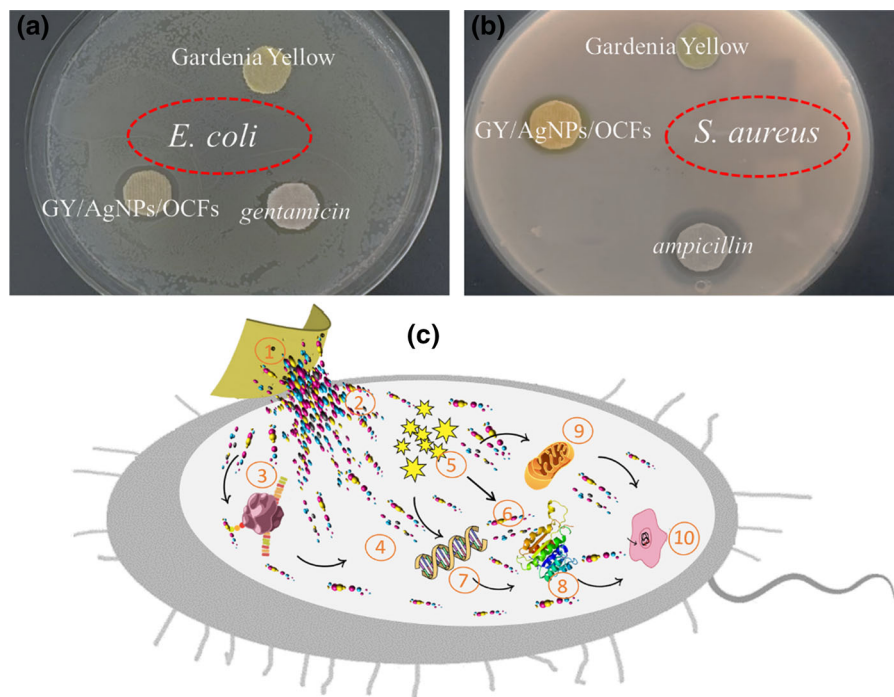


Fig. 7 Photographs of agar plate showing the antibacterial effect of samples against (a) *E. coli*, (b) *S. aureus*, and (c) possible mechanism of antibacterial action of AgNP dyed OCFs: ① AgNPs released by OCFs, ② cell membrane damage,

③ inhibition of electron transport chain, ④ destabilization of ribosomes, ⑤ formation of ROS, ⑥ oxidative stress, ⑦ damage of DNA, ⑧ damage of protein, ⑨ dysfunction of mitochondria, and ⑩ cell death

the cell membrane becomes damaged, and cell integrity is disrupted, and eventually, cell death happens. Another report has demonstrated that AgNPs can interact with the protein parts of the outer cell membrane. Then it makes complexes with oxygen, phosphorus, nitrogen, and sulfur atom and causes an irreversible change in the cell wall (Ghosh et al. 2012). The interaction of sulfur-containing membrane with AgNPs leads to the deactivation of bacterial growth (Lok et al. 2007). It also decreases the enzymatic activity of the respiratory chain of dehydrogenases in AgNP treated surface. Consequently, AgNPs damage the cell membrane, enter into the cell, and dehydrogenase the respiratory chain leading to cell death. (Roy et al. 2019). A mechanism of the bacterial effect of AgNP dyed OCFs against bacteria is proposed in Fig. 7c.

Conclusion

A straightforward and cost-effective traditional heating technique is explored here for the coloration and

simultaneous functionalization (bacterial resistance and UV protection) of OCFs via *in-situ* synthesis of AgNPs in natural dyes template extracted from gardenia yellow. The Taguchi model was used for statistical analysis in terms of signal to noise (S/N) ratios, main effect plots, interaction plots, residual plots, and fitted line plots at four levels on double signals (K/S and ΔE value). Experiments were conducted under the predicted optimal conditions to affirm the validity of the findings, and the results were in proper alignment with the predicted response. The surface plasmon property of AgNP imparted brilliant color on OCFs with strong color strength and fastness. The molecular force developed by plant phytochemicals and its double networking phenomenon via chemical linkage had enabled the successful fixation of particles. The protocol is highly effective for simultaneous functionalization in terms of antibacterial action and UV protection. Overall, natural dye reduced *in-situ* AgNPs on the OCFs surface-induced significant color and multi-functionality, thus overcoming the drawbacks of the traditional dyeing and finishing process.

Acknowledgements The authors thank the kind support of this work from Key Laboratory of Biomass Fibers & Eco-Dyeing and Finishing, Hubei Province (STRZ2020001) and Hubei Intellectual Property Office (2019044). The authors also thank Dr. S M Fijul Kabir (Department of Textile Engineering, Chemistry and Science; Wilson College of Textiles, North Carolina State University, Raleigh, NC 27695-8301, USA.) for his kind assistance in revision.

Declarations

Conflict of interest There is no conflict of interest in this paper.

References

- Aladpoosh R, Montazer M, Samadi NJC (2014) In situ green synthesis of silver nanoparticles on cotton fabric using *Seidlitzia rosmarinus* ashes. *Cellulose* 21:3755–3766. <https://doi.org/10.1007/s10570-014-0369-1>
- Cai X et al (2015) Optimization of ultrasound-assisted extraction of gardenia fruit oil with bioactive components and their identification and quantification by HPLC-DAD/ESI-MS². *Food Funct* 6:2194–2204. <https://doi.org/10.1039/C5FO00205B>
- Cai Y, Liang Y, Navik R, Zhu W, Zhang C, Pervez MN, Wang Q (2020) Improved reactive dye fixation on ramie fiber in liquid ammonia and optimization of fixation parameters using the Taguchi approach. *Dyes Pigm* 183:108734. <https://doi.org/10.1016/j.dyepig.2020.108734>
- Chae Y, Lee M, Cho G (2011) Mechanical properties and tactile sensation of naturally colored organic cotton fabrics. *Fibers Polym* 12:1042–1047. <https://doi.org/10.1007/s12221-011-1042-z>
- Chen J, Liu Y, Xiong Y, Wei D, Peng J, Mahmud S, Liu H (2021a) Konjac glucomannan reduced-stabilized silver nanoparticles for mono-azo and di-azo contained wastewater treatment. *Inorg Chim Acta* 515:120058. <https://doi.org/10.1016/j.ica.2020.120058>
- Chen J et al (2021b) Green synthesis of Konjac glucomannan templated palladium nanoparticles for catalytic reduction of azo compounds and hexavalent chromium. *Mater Chem Phys* 267:124651. <https://doi.org/10.1016/j.matchemphys.2021.124651>
- Chen J, Wei D, Liu Y, Xiong Y, Peng J, Mahmud S, Liu H (2020a) Gold/Konjac glucomannan bionanocomposites for catalytic degradation of mono-azo and di-azo dyes. *Inorg Chem Commun* 120:108156. <https://doi.org/10.1016/j.inoche.2020.108156>
- Chen Z et al (2020b) Hierarchical poly(vinylidene fluoride)/active carbon composite membrane with self-confining functional carbon nanotube layer for intractable wastewater remediation. *J Membr Sci* 603:118041. <https://doi.org/10.1016/j.memsci.2020.118041>
- Čuk N, Šala M, Gorjanc M (2021) Development of antibacterial and UV protective cotton fabrics using plant food waste and alien invasive plant extracts as reducing agents for the in-situ synthesis of silver nanoparticles. *Cellulose* 28:3215–3233. <https://doi.org/10.1007/s10570-021-03715-y>
- Durán N, Durán M, De Jesus MB, Seabra AB, Fávoro WJ, Nakazato G (2016) Silver nanoparticles: a new view on mechanistic aspects on antimicrobial activity. *Nanomed Nanotechnol Biol Med* 12:789–799. <https://doi.org/10.1016/j.nano.2015.11.016>
- Gengan R, Anand K, Phulokdaree A, Chuturgoon A (2013) A549 lung cell line activity of biosynthesized silver nanoparticles using *Albizia adianthifolia* leaf. *Coll Surf B* 105:87–91. <https://doi.org/10.1016/j.colsurfb.2012.12.044>
- Ghosh S et al (2012) Synthesis of silver nanoparticles using *Dioscorea bulbifera* tuber extract and evaluation of its synergistic potential in combination with antimicrobial agents. *Int J Nanomed* 7:483. <https://doi.org/10.2147/IJN.S24793>
- Gorenšek M, Recelj P (2007) Nanosilver functionalized cotton fabric. *Text Res J* 77:138–141. <https://doi.org/10.1177/0040517507076329>
- Guerena M, Sullivan P (2003) Organic cotton production. Citeseer, <https://attra.ncat.org/attra-pub/cotton.html>
- Guo X, Mahmud S, Zhang X, Yu N, Hasan KF (2021) One-Pot green synthesis of Ag@AgCl nanoparticles with excellent photocatalytic performance. *Surf Innov* 9:277–284. <https://doi.org/10.1680/jsuin.20.00089>
- Gürses A, Açıkıldız M, Güneş K, Gürses MS (2016) Dyes and pigments: their structure and properties. *Dyes Pigm*. https://doi.org/10.1007/978-3-319-33892-7_2
- Habib MA, Pervez MN, Mahmud S, Khan MMR, Heng Q (2017) Macadamia integrifolia: a new source of natural dyes for textile colouration. *Asian J Chem* 29(7):1543–1548. <https://doi.org/10.14233/ajchem.2017.20560>
- Hasan K et al (2019) A novel coloration of polyester fabric through green silver nanoparticles (G-AgNPs@PET). *Nanomaterials* 9:569. <https://doi.org/10.3390/nano9040569>
- Hasan KF, Wang H, Mahmud S, Taher MA, Genyang C (2020a) Wool functionalization through AgNPs: coloration, antibacterial, and wastewater treatment. *Surf Innov* 9:25–36. <https://doi.org/10.1680/jsuin.20.00031>
- Hasan KMF, Wang H, Mahmud S, Genyang C (2020b) Coloration of aramid fabric via in-situ biosynthesis of silver nanoparticles with enhanced antibacterial effect. *Inorg Chem Commun* 119:108115. <https://doi.org/10.1016/j.inoche.2020.108115>
- Hasan KMF, Wang H, Mahmud S, Jahid MA, Islam M, Jin W, Genyang C (2020c) Colorful and antibacterial nylon fabric via in-situ biosynthesis of chitosan mediated nanosilver. *J Mater Res Technol* 9:16135–16145. <https://doi.org/10.1016/j.jmrt.2020.11.056>
- Hossain MY, Liang Y, Pervez MN, Ye X, Dong X, Hassan MM, Cai Y (2021) Effluent-free deep dyeing of cotton fabric with cacao husk extracts using the Taguchi optimization method. *Cellulose* 28:517–532. <https://doi.org/10.1007/s10570-020-03525-8>
- Huang L, Sun Y, Mahmud S, Liu H (2019) Biological and environmental applications of silver nanoparticles synthesized using the aqueous extract of *Ginkgo biloba* leaf.

- J Inorg Organomet Polym Mater 30:1653–1668. <https://doi.org/10.1007/s10904-019-01313-x>
- Iravani S, Korbekandi H, Mirmohammadi SV, Zolfaghari B (2014) Synthesis of silver nanoparticles: chemical, physical and biological methods. *Res Pharm Sci* 9:385
- Kim Y et al (2017) Environmentally sound textile dyeing technology with nanofibrillated cellulose. *Green Chem* 19:4031–4035. <https://doi.org/10.1039/C7GC01662J>
- Le Marechal AM, Križanec B, Vajnhandl S, Valh JV (2012) Textile finishing industry as an important source of organic pollutants. Organic pollutants ten years after the Stockholm convention-environmental and analytical update. *IntechOpen, Rijeka*, pp 29–54
- Liu Y, Huang L, Mahmud S, Liu H (2020) Gold nanoparticles biosynthesized using Ginkgo biloba leaf aqueous extract for the decolorization of azo-dyes and fluorescent detection of Cr (VI). *J Cluster Sci* 31:549–560. <https://doi.org/10.1007/s10876-019-01673-x>
- Lok C-N et al (2007) Silver nanoparticles: partial oxidation and antibacterial activities. *J Biol Inorg Chem* 12:527–534. <https://doi.org/10.1007/s00775-007-0208-z>
- Mahmud S, Pervez M, Habib M, Sultana M, Liu H (2018) UV protection and antibacterial treatment of wool using green silver nanoparticles. *Asian J Chem* 30:116–122. <https://doi.org/10.14233/ajchem.2018.20924>
- Mahmud S, Pervez MN, Hasan KF, Taher MA, Liu H-H (2019) In situ synthesis of green AgNPs on ramie fabric with functional and catalytic properties. *Emerg Mater Res* 8:623–633. <https://doi.org/10.1680/jemmr.19.00012>
- Mahmud S, Pervez N, Sultana MZ, Habib A, Hui-Hong L (2017a) Wool functionalization by using green synthesized silver nanoparticles. *Orient J Chem* 33:2198
- Mahmud S, Pervez N, Taher MA, Mohiuddin K, Liu H-H (2020) Multifunctional organic cotton fabric based on silver nanoparticles green synthesized from sodium alginate. *Text Res J* 90:1224–1236. <https://doi.org/10.1177/0040517519887532>
- Mahmud S, Sultana M, Pervez M, Habib M, Liu H-H (2017b) Surface functionalization of “Rajshahi Silk” using green silver nanoparticles. *Fibers* 5:35. <https://doi.org/10.3390/fib5030035>
- Marin S, Mihael Vlasceanu G, Elena Tiplea R, Raluca Bucur I, Lemnar M, Minodora Marin M, Mihai Grumezescu A (2015) Applications and toxicity of silver nanoparticles: a recent review. *Curr Top Med Chem* 15:1596–1604. <https://doi.org/10.2174/1568026615666150414142209>
- Morshed MN, Pervez MN, Behary N, Bouazizi N, Guan J, Nierstrasz VA (2020) Statistical modeling and optimization of heterogeneous Fenton-like removal of organic pollutant using fibrous catalysts: a full factorial design. *Sci Rep* 10:1–14. <https://doi.org/10.1038/s41598-020-72401-z>
- Natsuki J, Natsuki T, Hashimoto Y (2015) A review of silver nanoparticles: synthesis methods, properties and applications. *Int J Mater Sci Appl* 4:325–332. <https://doi.org/10.11648/j.ijmsa.20150405.17>
- Perkins WS (1996) Textile coloration and finishing, 1st edn. Carolina Academic Press, North Carolina, USA
- Pervez M, Shafiq F, Sarwar Z, Jilani MM, Cai Y (2018) Multi-response optimization of resin finishing by using a taguchi-based grey relational analysis. *Materials* 11:426. <https://doi.org/10.3390/ma11030426>
- Pervez MN, Inamdar UY, Talukder ME, Mahmud S, Habib MA, Kamruzzaman M, Cai Y (2017) Eco-friendly coloration of linen to ameliorate its practical approach. In: MATEC Web of Conferences, EDP Sciences, p 03002 doi: <https://doi.org/10.1051/mateconf/201710803002>
- Rao SS, Saptami K, Venkatesan J, Rekha PD (2020) Microwave-assisted rapid synthesis of silver nanoparticles using fucoidan: characterization with assessment of biocompatibility and antimicrobial activity. *Int J Biol Macromol* 163:745–755. <https://doi.org/10.1016/j.ijbiomac.2020.06.230>
- Rehan M, Barhoum A, Khattab TA, Gätjen L, Wilken R (2019) Colored, photocatalytic, antimicrobial and UV-protected viscose fibers decorated with Ag/Ag₂CO₃ and Ag/Ag₃PO₄ nanoparticles. *Cellulose* 26:5437–5453. <https://doi.org/10.1007/s10570-019-02497-8>
- Rieple A, Singh R (2010) A value chain analysis of the organic cotton industry: the case of UK retailers and Indian suppliers. *Ecol Econ* 69:2292–2302. <https://doi.org/10.1016/j.ecolecon.2010.06.025>
- Roy A, Bulut O, Some S, Mandal AK, Yilmaz MD (2019) Green synthesis of silver nanoparticles: biomolecule-nanoparticle organizations targeting antimicrobial activity. *RSC Adv* 9:2673–2702. <https://doi.org/10.1039/C8RA08982E>
- Ru J, Qian X, Wang Y (2018) Study on antibacterial finishing of cotton fabric with silver nanoparticles stabilized by nanoliposomes. *Cellulose* 25:5443–5454. <https://doi.org/10.1007/s10570-018-1953-6>
- Samanta P (2020) A review on application of natural dyes on textile fabrics and its revival strategy. In: Chemistry and technology of natural and synthetic dyes and pigments. *IntechOpen*: doi: <https://doi.org/10.5772/intechopen.90038>
- Sanchez RA, Takamune K, Guimarães B, Alonso R, Baruque-Ramos J, De Held MSB, Marcicano JPP (2014) Wearability Analysis of knited fabrics produced with colored organic cotton. Bamboo rayon, corn, recycled pet/cotton and recycled pet/polyester. *Am Int J Contemp Res* 4:28–37
- Saravanakumar K, Chelliah R, Shanmugam S, Varukattu NB, Oh D-H, Kathiresan K, Wang M-H (2018) Green synthesis and characterization of biologically active nanosilver from seed extract of *Gardenia jasminoides* Ellis. *J Photochem Photobiol B* 185:126–135. <https://doi.org/10.1016/j.jphotobiol.2018.05.032>
- Shafiq F, Pervez MN, Jilani MM, Sarwar Z, Hasani H, Cai Y (2018) Structural relationships and optimization of resin-finishing parameters using the Taguchi approach. *Cellulose* 25:6175–6190. <https://doi.org/10.1007/s10570-018-1957-2>
- Shahidul I, Butola BS, Kumar A (2020) Green chemistry based in-situ synthesis of silver nanoparticles for multifunctional finishing of chitosan polysaccharide modified cellulosic textile substrate. *Int J Biol Macromol* 152:1135–1145. <https://doi.org/10.1016/j.ijbiomac.2019.10.202>
- Shaikh MA (2009) Water conservation in textile industry. *Pak Text J* 58(11):48–51
- Shateri-Khalilabad M, Yazdanshenas ME, Etemadifar A (2017) Fabricating multifunctional silver nanoparticles-coated cotton fabric. *Arab J Chem* 10:S2355–S2362. <https://doi.org/10.1016/j.arabj.2013.08.013>

- Sultana MZ, Mahmud S, Pervez MN, Hasan KF, Heng Q (2019) Green synthesis of glycerol monostearate-modified cationic waterborne polyurethane. *Emerging Mater Res* 8:137–147. <https://doi.org/10.1680/jemmr.18.00022>
- Tavaf Z, Tabatabaei M, Khalafi-Nezhad A, Panahi F, Hosseini A (2015) Green synthesis of silver nanoparticles by reduced glycosylated casein adducts: assessment of their antibacterial and antioxidant activity against *Streptococcus mutans*. *Eur J Integr Med* 7:294–302. <https://doi.org/10.1016/j.eujim.2015.02.001>
- Thangaraj V, Mahmud S, Li W, Yang F, Liu H (2017) Greenly synthesised silver-alginate nanocomposites for degrading dyes and bacteria. *IET Nanobiotechnol* 12:47–51. <https://doi.org/10.1049/iet-nbt.2017.0074>
- Tian Y, Shu Y, Zhang X, Mahmud S, Zhu J, Su S (2020) Electrospun PVDF-Ag@AgCl porous fiber membrane: stable antifouling and antibacterial surface. *Surf Innov* 9:156–165. <https://doi.org/10.1680/jtsuin.20.00050>
- Vankar PS (2000) Chemistry of natural dyes. *Reson* 5:73–80. <https://doi.org/10.1007/BF02836844>
- Vasireddy R, Paul R, Mitra AK (2012) Green synthesis of silver nanoparticles and the study of optical properties. *Nanomater Nanotechnol* 2:8. <https://doi.org/10.5772/52329>
- Wan H, Li C, Mahmud S, Liu H (2021a) Kappa carrageenan reduced-stabilized colloidal silver nanoparticles for the degradation of toxic azo compounds. *Coll Surf B* 616:126325. <https://doi.org/10.1016/j.colsurfa.2021.126325>
- Wan H, Liu Z, He Q, Wei D, Mahmud S, Liu H (2021b) Bioreduction (Au^{III} to Au⁰) and stabilization of gold nanocatalyst using Kappa carrageenan for degradation of azo dyes. *Int J Biol Macromol* 176:282–290. <https://doi.org/10.1016/j.ijbiomac.2021.02.085>
- Wang H et al (2022) Bioreduction (Ag⁺ to Ag⁰) and stabilization of silver nanocatalyst using hyaluronate biopolymer for azo-contaminated wastewater treatment. *J Alloys Compd* 894:162502. <https://doi.org/10.1016/j.jallcom.2021.162502>
- Wang Z, Lü S, Yang F, Kabir SMF, Mahmud S, Liu H (2021) Hyaluronate macromolecules reduced-stabilized colloidal palladium nanocatalyst for azo contaminated wastewater treatment. *Coll Surf* 628:127345. <https://doi.org/10.1016/j.colsurfa.2021.127345>
- Xiong Y, Huang L, Mahmud S, Yang F, Liu H (2020) Biosynthesized palladium nanoparticles using alginate for catalytic degradation of azo-dyes. *Chin J Chem Eng* 28:1334–1343. <https://doi.org/10.1016/j.cjche.2020.02.014>
- Xiong Y et al (2021) Hyaluronate macromolecules assist bioreduction (Au^{III} to Au⁰) and stabilization of catalytically active gold nanoparticles for azo contaminated wastewater treatment. *Environ Technol Innov* 24:102053. <https://doi.org/10.1016/j.eti.2021.102053>
- Xu W, Yu J, Feng W, Su W (2016) Selective extraction of gardenia yellow and geniposide from *Gardenia jasminoides* by mechanochemistry. *Molecules* 21:540. <https://doi.org/10.3390/molecules21050540>
- Yazdanshenas ME, Shateri-Khalilabad M (2012) The effect of alkali pre-treatment on formation and adsorption of silver nanoparticles on cotton surface. *Fibers Polym* 13:1170–1178. <https://doi.org/10.1007/s12221-012-1170-0>
- Yu Z, He H, Liu J, Li Y, Lin X, Zhang C, Li M (2019) Simultaneous dyeing and deposition of silver nanoparticles on cotton fabric through in situ green synthesis with black rice extract. *Cellulose* 27:1829–1843. <https://doi.org/10.1007/s10570-019-02910-2>
- Zhang X et al (2021) Sodium alginate fasten cellulose nanocrystal Ag@AgCl ternary nanocomposites for the synthesis of antibacterial hydrogels. *Compos Commun* 25:100717. <https://doi.org/10.1016/j.coco.2021.100717>
- Zhou S, Wang W, Sun Y, Tang X, Zhang B, Yao X (2021) Antibacterial effect of Ag-PMANa modified cotton. *Coll Surf A* 618:126453. <https://doi.org/10.1016/j.colsurfa.2021.126453>

Publisher's Note Springer Nature remains neutral with regard to jurisdictional claims in published maps and institutional affiliations.